DOI: 10.13009/EUCASS2019-425

Characterization of dynamic hydroplaning speed for large transport aircraft equipped with a multi-row main landing gear

Sara Lagunas Caballero
Airbus Defence & Space
Paseo de John Lennon s/n, Getafe, Spain
sara.lagunas@airbus.com

Abstract

In the context of ground operations on water contaminated runways, hydroplaning constitutes a critical condition, which leads to strong wheel spin-down and substantial loss of braking friction, and may result in undesired runway excursions. Therefore, an adequate knowledge of the ground speed at which dynamic hydroplaning starts to develop (hydroplaning speed, V_p) becomes essential.

EASA (AMC 25.1591) and FAA (AC 25-31) accept the characterization of V_p as a sole function of tire inflation pressure (p), by means of formula $V_p = 9\sqrt{p}$ (V_p in kt, p in psi). Such relation was established in 1963, based on the results of ten unique test points. This paper attempts to bring into question the relevance of this relation. Additionally, neither EASA nor the FAA allow for the consideration of a variation in the hydroplaning definition above in multi-row undercarriages, in which not all wheels are equally affected by the contaminant: front wheels both displace fluid from the path of aft wheels and impinge fluid on them. Therefore, a non-negligible variation in V_p might be found.

Another aspect assumed by the aforementioned advisory material is that, in terms of braking performance, hydroplaning conditions are analogous to icy ones, accepting a characteristic braking friction value of 0.05.

The present study pursues two different objectives. The first is to assess the differences in the onset of hydroplaning depending on wheel position (front or aft). The second is to evaluate if the advisory braking friction proposed by EASA and the FAA to be applied in hydroplaning conditions, is adequate for multi-row MLG assemblies.

A series of taxi tests were conducted on a specifically built pond facility, simulating highly contaminated conditions (15 mm water on average) in support of the study. The selected test aircraft was equipped with a dual-tandem MLG. All tests were performed on the same runway, of sufficient macro texture to provide adequate drainage. All tires had equal type, dimensions, and inflation pressures, and were circumferentially grooved. The ground speed (Vg) range covered was 60-110 kt. The criterion established for the detection of V_p was a combination of wheel spin-down and residual to null braking torque. Both parameters were monitored at 128 Hz.

Hydroplaning was apparent on front wheels from 100 kt. Nevertheless, no spin-down was observed on aft wheels, and their braking torque was not as highly degraded.

Results suggest that the MLG configuration plays a part in the onset of hydroplaning at aircraft level, and it therefore may be considered as an additional parameter for the characterization of V_p. At front wheel level, the observed correlation between tire inflation pressure and V_p was $V_p = 8.4\sqrt{p}$. In contrast, aft wheels did not reach hydroplaning over the entire ground speed range tested.

Further hydroplaning-dedicated testing is recommended, with a view to provide further evidence to support a review of the current certification standards.

Keywords: Contaminated Runways, Hydroplaning, Dual-Tandem, Multi-Row Main Landing Gear.

DOI: 10.13009/EUCASS2019-425

1. Introduction

Dynamic hydroplaning is the phenomenon in which a tire passing at high speed over a surface covered with a fluid contaminant (standing water, slush, or wet snow) loses contact with the ground, and is entirely sustained by the fluid layer. Since fluids cannot develop relevant shear forces, both tire traction and tire-to-ground friction drop to values significantly lower than those encountered on dry surfaces. Hydroplaning conditions are therefore critical, and highly prone to resulting in undesired runway excursions, particularly upon landing.
Civil regulations (Ref. [1], Ref. [2]) propose a characterization for dynamic hydroplaning speed (V_p), as part of their advisory material. Nevertheless, several areas of improvement have been identified. Firstly, this speed is characterized as a single value of ground speed, dependent solely on tire inflation pressure. Secondly, no distinction is made between hydroplaning development at tire and aircraft level, hindering the applicability of this model on aircraft equipped with multi-row Main Landing Gear (MLG) arrangements. Finally, accepted braking friction value in hydroplaning conditions is 0.05, regardless of the undercarriage configuration considered.
The present work proposes a flight test based re-evaluation of dynamic hydroplaning speed models for multi-row MLG aircraft, as well as an analysis of braking performance deterioration under such conditions. Results are put into context by means of comparison with regulatory models and state-of-the-art algebraic characterizations.

2. Hydroplaning Speed

2.1 Definition

Hydroplaning was identified as a problem related with aircraft operations back in the 1940s-50s, when significant increases in ground speed where achieved following World War II. At the time, operations and tests were carried out on runways with approximate average macrotexture depths of 0.25 mm (Class B/C surfaces), no longer representative of drainage capabilities of modern runway surfaces, which can reach macrotexture depths of 1 to 2 mm (Class D/E surfaces) (Ref. [3]).
Out of the three types of hydroplaning (dynamic, viscous and reverted rubber), dynamic hydroplaning constitutes the most common condition. It takes place when hydrodynamic lift force (L_h) generated by the contaminant layer equals the total normal load exerted by the tire on the ground (N_w).

$$L_h = N_w \tag{1}$$

Normal load can be approximated as the product of tire inflation pressure p and a reference contact surface with the ground, S_{ref}

$$N_w \approx p\, S_{ref} \tag{2}$$

As any fluid dynamic force, the hydrodynamic lift generated is proportional to the fluid dynamic pressure, and therefore, to the square of the relative speed between tire and fluid; that is, ground speed (Vg).

$$L_h = \frac{1}{2}\rho_c Vg^2 S_{ref} C_{Lh} \tag{3}$$

The ground speed at which hydrodynamic lift outbalances overall download force on the wheel is called **hydroplaning speed** (V_p). Matching the two above equations for $GS = V_p$, hydroplaning speed can be expressed as proportional to the square root of tire inflation pressure:

$$V_p \approx K\sqrt{p} \tag{4}$$

Following this scheme, NASA published, in 1963, the subsequent correlation for hydroplaning speed of rib-tread tires on **water** flooded surfaces (V_p in kt, p in psi) (Ref. [6]):

$$V_p = 9\sqrt{p} \tag{5}$$

This relation was obtained from the analysis of **ten** unique test points. In addition to this, no information is provided about the phenomena chosen to identify when the onset of hydroplaning took place. Despite its "obscurity", this formula has been used as a basis for the characterization of hydroplaning speed on the advisory material of European (EASA AMC 25.1591) and American (FAA AC 25-31) Certification Standards.

DOI: 10.13009/EUCASS2019-425

2.2 Definition

The onset of dynamic hydroplaning can be identified by two conditions: strong wheel spin-down and loss of tire-to-ground contact. Spin–down is a consequence of tire deformation, and subsequent displacement of its center of pressure a certain forward distance x_c from the wheel axle. As a result, hydrodynamic lift exerts a large contra-rotatory moment on the wheel, that can lead to stopping or even reversal of wheel rotation. On its behalf, loss of contact between tire footprint and runway leads to drastic reductions in both tire directional stability and braking friction (Figure 1).

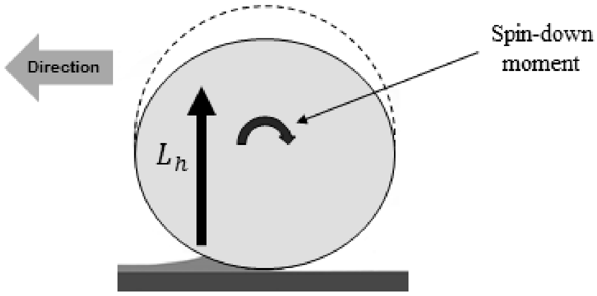

Figure 1: Schematic representation of tire undergoing dynamic hydroplaning

Some authors assert that the aforementioned conditions are not necessarily simultaneous (Ref. [3]). Indeed, it is suggested that they are indicative of two different degrees of dynamic hydroplaning: *partial* (associated to strong spin-down and residual tire-to-ground contact) and *complete* (associated to full wheel detachment from the ground). In that case, a single value of hydroplaning speed would not be sufficient to properly characterize the hydroplaning phenomenon. Consequently, it is proposed to consider two different hydroplaning speeds: partial (denoted as V_S) and complete (denoted as V_H).

2.3 Hydroplaning Speed Models

2.3.1 Civil Regulations

As stated, AMC 25.1591 accepts the characterization of V_p for water flooded surfaces as $V_p = 9\sqrt{p}$ (Ref. [1]). Therefore, tire pressure is regarded as the sole variable of influence. According to this material, the result of reaching ground speeds beyond the aforementioned is a reduction in braking friction coefficient to a value of 0.05. In order to provide some context, this corresponds to the reference value for friction on icy conditions considered by EASA.
The last issue of AC 25-31, published on December 2015 takes advantage of the same V_p characterization. Nevertheless, it introduces the notion that braking friction sinking does not start at $V_p = 9\sqrt{p}$, but at a slightly lower speed, that will be denoted as V_b, such that $V_b = 0.85V_p$.

2.3.2 Algebraic Models

2.3.2.1 Variables of Influence

In 2015, (Ref. [3], Ref. [4]) proposed a characterization of hydroplaning speed based on properties of the three elements that are directly involved in the hydroplaning phenomenon: tire, runway surface, and contaminant between them. Tire-related properties include dimensions (diameter (D) and width (w)), tread type (ribbed or smooth) and inflation pressure (p). Runway surface is characterized by its macro texture depth (d_{TEX}). Macro texture is the visible roughness of a surface, formed by the presence of stones or grooves. Its main function is to enhance drainage of fluid contaminants, by creating channels which this fluid to escape. Finally, contaminant is represented by its density (ρ_C) and depth (d_C).

DOI: 10.13009/EUCASS2019-425

2.3.2.2 Analytical model

Ref. [5] proposes an algebraic model for the characterization of displacement drag at tire level. Some interesting concepts can be extracted from this analysis. The first is the introduction of a certain drainage parameter (τ), which models drainage capability as a function of contaminant (d_C) and macro texture (d_{TEX}) depths.

$$\tau = 1 + \frac{d_{TEX}}{d_C} \tag{6}$$

High τ values are indicative of high drainage capability, which shall translate into higher hydroplaning speeds. As can be seen, high d_{TEX} values increase τ. It should be remarked that this parameter does not take into account the non-negligible contribution to drainage of tire tread pattern. This is because the influence of tire tread is considered separately, by means of a set of constants c_{ij}. Table 1 specifies the proposed values for ribbed tires.

Table 1: c_{ij} constants for ribbed tires

	c_{01}	c_{10}	$\boldsymbol{c_{11}}$	$\boldsymbol{c_{12}}$
Ribbed tire	0.2661	0	1.52	0.3125

The previous are then combined with tire fineness ratio (defined as the quotient between its width and its diameter, w/D) to conform constants c_0 and c_1:

$$c_0 = \left(\frac{w/D}{c_{01}}\right)^2 \tag{7}$$

$$c_1 = c_{10} + \frac{c_{11}}{1+\left(\frac{w/D}{c_{12}}\right)^2} \tag{8}$$

Taking advantage of the previous, Ref. [3] proposes a theoretical model for the estimation of partial (V_S) and complete (V_H) hydroplaning speeds.
Partial hydroplaning speed (V_S) is modelled as:

$$V_S = \left(\frac{c_1 \tau^2 \pi p}{\rho_C (\tan^{-1}(0.95))^{1/2}}\right)^{1/2} \tag{9}$$

Complete hydroplaning speed (V_H) is modelled as:

$$V_H = \tau \left(\frac{\pi p}{\rho_C}\right)^{1/2} \tag{10}$$

According to this formulation, $V_S < V_H$, which means that spin-down is assumed to precede tire detachment from the ground. Additionally, important conclusions can be extracted. First of all, both V_S and V_H are proportional to the term $\tau(\pi p/\rho_C)^{1/2}$, which means that contaminant and runway features influence all degrees of hydroplaning speed. Secondly, tire geometry and tread characteristics have an influence on V_S, but not on V_H. Assuming that the above model accurately represents hydroplaning physics, the straightforward conclusion would be that the selection of tires of adequate geometry and tread pattern could retard the development of partial hydroplaning, but would by no means affect the onset of complete hydroplaning. Finally, it is important to emphasize that none of these models take into account the position of the wheel relative to the other wheels in the bogie row astern position as a factor in hydroplaning characterization.

DOI: 10.13009/EUCASS2019-425

3. Design of Test Campaign

The test strategy comprised a series of full-pedal braked taxi tests performed at constant ground speed over a water contaminated runway. The ground speed range covered was 60 to 110 kt, so as to ensure sufficient lower and upper margin with respect to hydroplaning speed. A build-up approach was adopted in terms of speed, beginning with the lowest values of ground speed and increasing them gradually in each subsequent test. The speed increment considered was 10 kt, in order to achieve the best possible compromise between adequate speed control and reasonably precise detection of hydroplaning speed. For all tests, an average water depth of 15 mm (the maximum contemplated by AMC 25.1591) was ensured.

3.1 Test Aircraft

A heavy transport aircraft, with an approximate weight of 110 t, was selected for testing. The main landing gear (MLG) consists of two symmetric assemblies, respectively attached to the left and right sides of the lower central fuselage.
For this investigation, a focus on the dual-tandem layout (two wheels abreast, two pairs in a row) was considered. Figure 2 shows a schematic representation of the former.

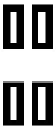

Figure 2: Schematic representation of dual-tandem landing gear assembly

All tires are identical, and follow a bias-ply construction, with dimensions 43x15.5-17, and circumferentially grooved. As per test requirement, they were neither new nor worn at the time of testing, with groove depths 10% to 90% of the allowable range. Inflation pressure was carefully controlled, and equal to 140±2 psi.

3.2 Test facilities

The runway selected for the test campaign presented an average macro texture depth of 1.4 mm (Class E surface). Contaminated conditions were simulated by means of two specifically built ponds, each 100 m long x 5 m wide, and located 1.15 m away from the runway centerline (Figure 3). Nose landing gear interaction with the contaminant was out of the scope of the investigation.

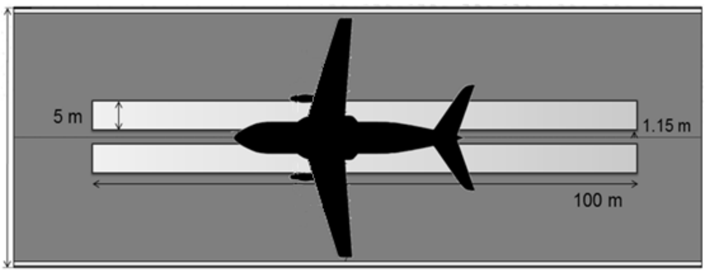

Figure 3: Schematic representation of pond facilities (including dimensions)

Due to the runway slope, water tended to accumulate at the exit of the pond, which made it difficult to maintain a uniform depth along the contaminated area. The solution for this issue was to divide each pond in a series of sub-ponds along its length. As shown in Figure 4, 13 sections (each 7.7 m long) were considered. This design does not completely prevent water from accumulating at the exit of each section, but permits to keep a more uniform depth along the pond. Furthermore, since sub-ponds are “isolated” from one another, the pass of the plane only has an effect on the water contained in the sub-pond where the plane is located in that instant, but not in the adjacent ones. This leads to a reasonable agreement between the local depth values calculated from the initial measurements and those actually experienced by the front wheels.

DOI: 10.13009/EUCASS2019-425

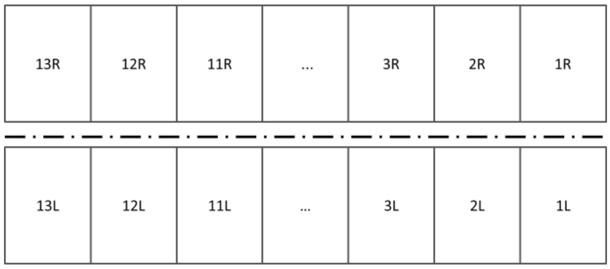

Figure 4: Pond subdivisions

A metal ring and a water depth gauge were utilized to measure depths at two points in each sub-pond, located over the expected aircraft trajectory (Figure 5). Such values were then extrapolated to the totality of the pond, using local values of transversal and longitudinal slope at each sub-pond. This permitted both to check that the intended average depth had been attained, and to have a precise estimation of local depth variations.

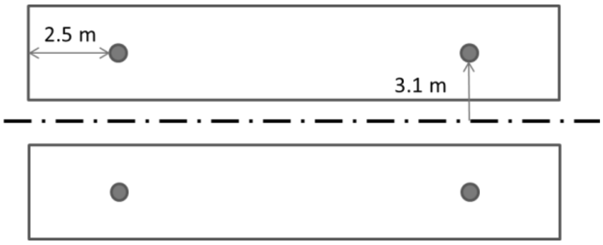

Figure 5: Position of depth measurement points within each sub-pond

3.3 Depth Tracking

Table 2 shows average local depth encountered at inner and outer MLG abreast positions.

Table 2: Average Depth Measurements

Test Ground Speed (kt)	Inner Depth (mm)	Outer Depth (mm)
60	13	25
70	13	25
80	17	28
90	16	27
100	12	23
110	17	28

Such values are representative for front tires only. Due to contaminant displacement exerted by these, as well as contaminant impingement among MLG wheels, it is not possible to accurately estimate actual depths encountered by every wheel. As can be seen, local depth differences between wheels are not negligible, but are consistent among the different tests, which simplifies the analysis. Right outer wheel is subjected to the highest depths, which can be 5 to 10 mm higher than those experienced by right inner wheel.

DOI: 10.13009/EUCASS2019-425

4. Test Based Hydroplaning Speed Characterization

4.1 Criteria for Identification of Hydroplaning Onset

Following the strategy proposed by Ref. [3], the criterion for hydroplaning speed identification will be based on variables that allow for a straightforward detection of wheel spin-down and loss of braking friction.
Slip ratio (SR) is the parameter of choice for spin-down detection. It relates wheel rotational speed (ωR) with vehicle ground speed (Vg), as follows:

$$SR = 1 - \frac{\omega R}{Vg} \quad \textbf{(11)}$$

In order to provide some context for this parameter, some reference values might be helpful. $SR = 0$ represents a free-rolling condition, in which ωR equals Vg. $SR = 1$ represents a full slippage condition, in which no rolling takes place. Nominal SR values for optimum braking are in the range 0.1-0.15, but they might be subjected to variations depending on operating conditions; in particular, the presence of contaminants on the runway. In general, a *continuously growing* evolution of SR values in the range [0.5-1] is indicative of strong spin-down. Aircraft ground speed, as well as rotational speed and normal load applied on each wheel were monitored at 128 Hz. Actual wheel radius was calculated at each time instant, considering both nominal radius and tire deflection due to the aforementioned normal load.
Braking torque (SR) is the parameter of choice for identification of braking performance deterioration. As shown by its name, this torque is generated by the brakes, and is opposite to wheel rotation (Figure 6). It generates a horizontal reaction ($F_{braking}$, braking force) contrary to wheel direction of motion, which eventually stops the vehicle. Therefore, the evolution of braking torque allows for a straightforward assessment of wheel braking performance. As for rotational speed and normal load, braking torque exerted on each wheel was also monitored at 128 Hz.

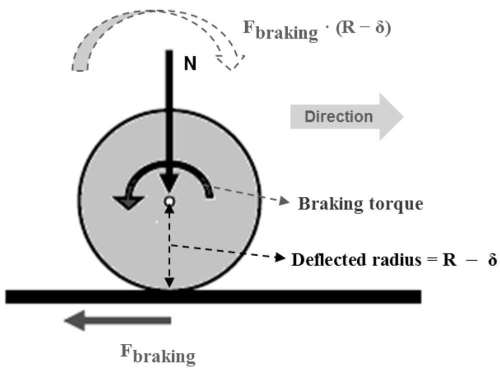

Figure 6: Braking process on a wheel

4.2 Hydroplaning Speed at Front Wheels

The front wheels are the ones subjected to the most critical conditions, since they are responsible for bulk fluid displacement and are not sheltered from the contaminant by any forward wheels.

4.2.1 Slip Ratio Evolution

Figure 7 shows the evolution of slip ratio for front wheels at Vg 60-100 kt. As can be seen, from 60 to 90 kt, the wheels do not experience significant increases in slip ratio. Nevertheless, at 90 kt, incipient spin-down is evident at inner wheel. From 100 kt on, strong spin-down is present in all front wheels.

DOI: 10.13009/EUCASS2019-425

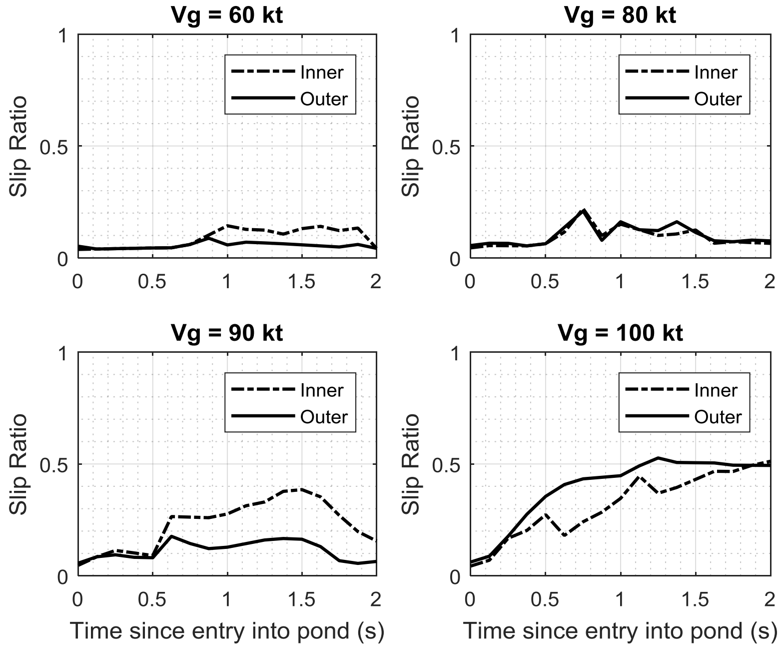

Figure 7: Slip Ratio Evolution on Front Wheels

4.2.2 Braking Torque Evolution

Figure 8 is analogous to figure 7, but now showing the evolution of non-dimensional braking torque. At 60 kt, the expected levels of braking torque can be found in all wheels. Nevertheless, at 80 kt, the braking torque is reduced to a residual level. From 90 kt onward, braking torque becomes negligible.

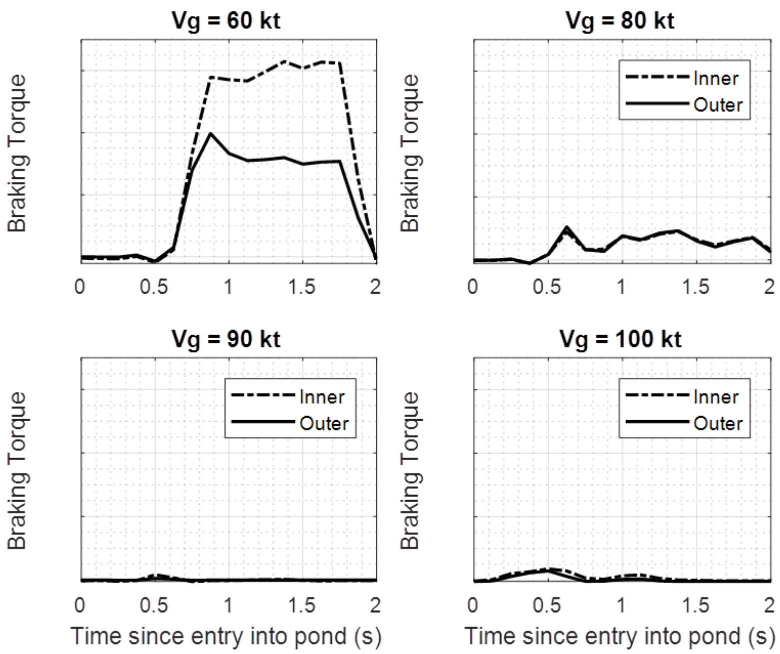

Figure 8: Braking Torque Evolution on Front Wheels

DOI: 10.13009/EUCASS2019-425

4.2.3 Discussion

Ref. [3] and Ref. [4] assume spin-down to be indicative of partial hydroplaning, loss of braking capability to be indicative of complete hydroplaning, and the former to take place at a lower sped than the latter. Nevertheless, the above results show that braking torque was residual-to-null at 90 kt; that is, around 10 kt before spin-down is evident. This might be indicative of hydroplaning not being a progressive phenomenon in the way described by previous references. Significant reduction in braking torque is shown to be simultaneous, if not prior, to noticeable spin-down.
In the light of these results, an appropriate characterization strategy could be one similar to that followed by the last issue of AC 25-31 (Ref. [2]), presented at Section 2.3.1. As a result, it is possible to distinguish two speeds: V_b(braking loss speed) at approximately 90 kt, and V_p (complete planing speed) at approximately 100 kt.

4.3 Hydroplaning Speed Characterization at Aft Level

4.3.1 Slip Ratio Evolution

Figure 9 shows the evolution of slip ratio for all MLG wheels at two different ground speeds: 70 kt, before front wheels reach hydroplaning, and 110 kt, when the complete front row is fully detached from the ground. As shown, and unlike front wheels, aft wheels do not experience significant increases in slip ratio, aside from occasional, instantaneous peaks that are rapidly recovered. In other words, no spin-down is detected along the speed range tested.

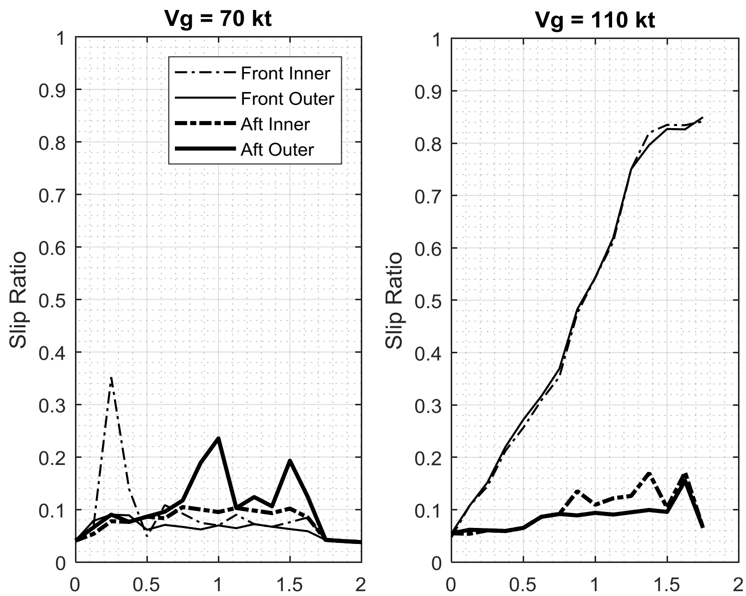

Figure 9: Comparison of Slip Ratio evolution between front and aft wheels

4.3.2 Braking Torque Evolution

Figure 10 is analogous to the previous one, but now comparing the evolution of braking torque. Again, aft wheels are capable of generating reasonable braking torque values, which are by no means representative of the residual shear forces that would be generated by a tire fully sustained by a fluid layer. In other words, aft row does not detach from the ground although the front row clearly does.

DOI: 10.13009/EUCASS2019-425

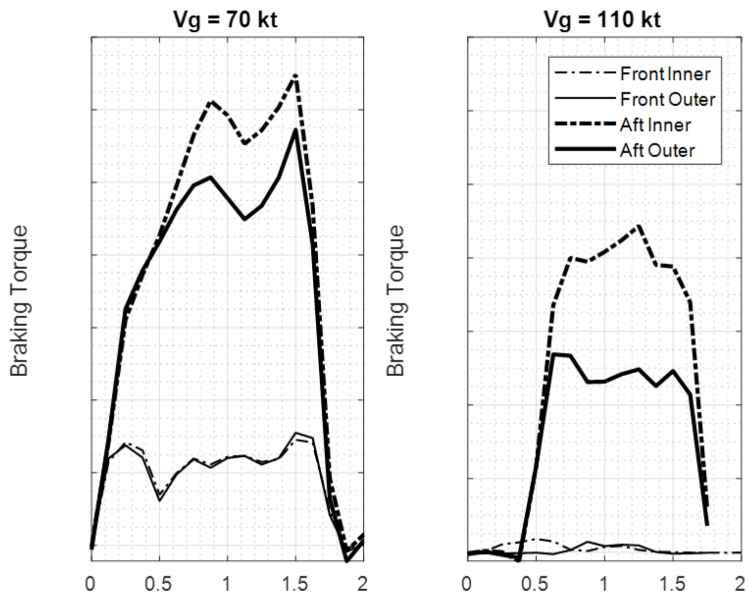

Figure 10: Comparison of Braking Torque evolution between front and aft wheels

4.3.3 Discussion

The above constitutes evidence that mid and aft wheels do not meet any of the conditions associated to either partial or complete hydroplaning over the Vg range tested, not even when front wheels are fully affected by this condition. Two conclusions can be extracted. First, a single hydroplaning speed value (based on front row) is not representative for full aircraft hydroplaning on multi-row MLG arrangements. Second, the configuration of the wheels on the bogie should be taken as an additional factor for the characterization of hydroplaning speed.

4.4 Results Comparison

Table 3 compares the test-derived hydroplaning speed with the values proposed by the theoretical and regulatory models presented in Section 2.

Table 3: Comparison of hydroplaning speed values

	V_b (kt)	V_S (kt)	V_H *or* V_P(kt)
AMC 25.1591	-	-	106.5
AC 25-31	90.5	-	106.5
ESDU 15003	-	81	114
Tests (front wheels)	90 [a]	-	100 [a]
Tests (aft wheels)	>110[b]	-	>110[b]

[a] Approximate values, due to 10 kt testing interval
[b] Highest Vg tested

DOI: 10.13009/EUCASS2019-425

The following observations can be made: The first and most important is that tests are strongly indicative that wheel astern position plays a role in hydroplaning development that may not be insignificant. The second is that the hydroplaning process observed in the tests does not seem to follow the partial-to-complete build-up proposed by Ref. [3], but the one suggested by AC 25-31, in which loss of braking friction precedes wheel hydroplaning. Test-derived $V_b$is very close to that proposed by AC 25-31. Nevertheless, test-derived full hydroplaning speed is lower than that predicted by both advisory material and the ESDU 15003 algebraic model. Finally, according to test results, V_p can be more closely correlated with inflation pressure as $V_p = 8.4\sqrt{p}$.

5. Braking Performance Deterioration

According to both AMC 25.1591 and AC 25-31, braking conditions in hydroplaning conditions are comparable to those found in icy environments, in which a residual braking friction coefficient of 0.05 is accepted as valid. As shown in Section 4.2, this might accurately describe the behaviour of front wheels, which reach negligible braking torque levels after hydroplaning is developed, and only residual ones at slightly lower speeds. Nevertheless, as shown by Section 4.3.2, this does not seem to be the case for aft wheels.

Figure 11 compares the evolution of braking torque levels at front and aft wheels over the ground speed range tested. Results are indicative that braking torque levels at aft wheels observed in aft wheels are substantially higher to those observed in front ones, even at ground speed values at which front wheels experience complete planing. Moreover, observed braking torque levels on aft wheels at 100 and 110 kt (beyond front wheel hydroplaning speed) are substantially higher than those reached by front wheels at 70 kt, well before hydroplaning starts to develop. This suggests that braking torque degradation suggested by AMC 25.1591 and AC 25-30 might be overly conservative, and therefore not representative, multi-wheel bogie arrangements.

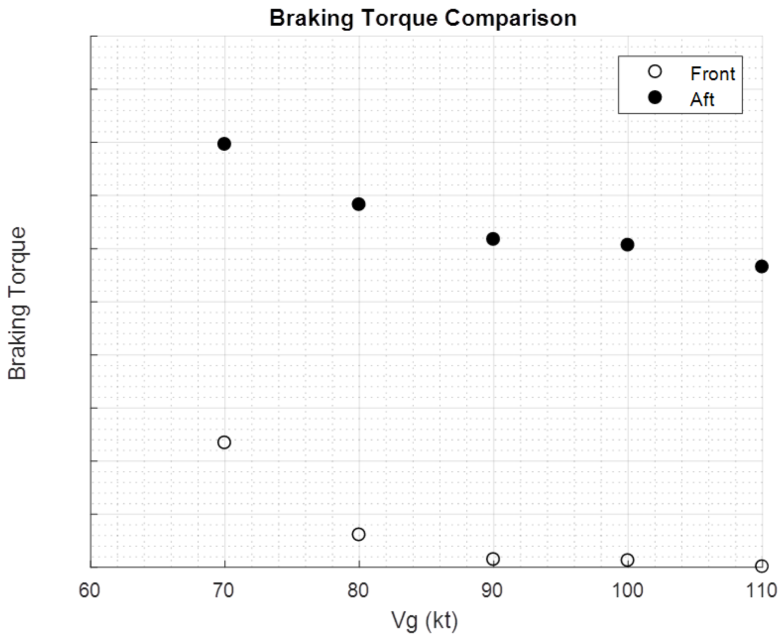

Figure 11: Comparison of Braking Torque evolution in front and aft wheels

DOI: 10.13009/EUCASS2019-425

6. Conclusions and Future Work

Three relevant conclusions can be extracted. First of all, the relative wheel position in a multi-wheel bogie seems to play a key role in the development of hydroplaning. As a result, a single hydroplaning speed value is not representative of overall aircraft when a multi-row undercarriage is considered. Secondly, observed hydroplaning speeds at front tire level are slightly lower than those proposed by theoretical and regulatory models. Finally, the braking capability of aft wheels once the front tires reach hydroplaning is by no means negligible, and may even be considerably greater that that observed on the front tires below hydroplaning conditions.
Future work should include further hydroplaning-dedicated testing at both tire and full landing gear levels, with a view on a prospective update of current certification standards.

Acknowledgements

The author would like to thank Airbus D&S Aircraft Performance Domain; in particular Dr. Giel Cohen for his continuous commitment to innovation, and Mr. Raúl Torres Aparicio, for his vast engineering knowledge and his excellent mentoring in the last three years.

Thanks to my colleagues Mr. Félix Delgado Ferreirós, Mr. Ricardo Lissen Pérez, Mr. Diego Sánchez Franco and Mr. Vinicius Ayello Deo.

Thanks to my parents, uncle, aunt, and of course Esther Lagunas and Pablo Gumiel.

References

[1] EASA. CS-25 AMC 25.1591. The derivation and methodology of performance information for use when taking-off and landing with contaminated runway surface conditions.
[2] FAA. 2015. AC 25-31. Takeoff Performance Data for Operations on Contaminated Runways, Issued December 2015.
[3] ESDU. 2015. Planing of rib-tread aircraft tyres. ESDU 15003, London, Issued June 2015 (with Amendment A, July 2016).
[4] ESDU. 2016. Determination of hydroplaning speeds and corresponding hydrodynamic forces for rib tread aircraft tyres. Application of ESDU 15003. ESDU 15009, London, Issued July 2016.
[5] ESDU. 2013. Model for performance of a single aircraft tyre rolling or braking on dry or precipitate contaminated runways. ESDU 10015, London, Issued February 2013 (with Amendment A, November 2013).
[6] Horne, W.B., Dreher, R.C. Phenomena of pneumatic tyre hydroplaning. NASA Technical Note, NASA TN D-2056, Issued November 1963.